

The Same but Different – Cell Intercalation as a Driver of Tissue Deformation and Fluidity

Robert J. Tetley¹, Yanlan Mao^{1, 2, 3*†}

¹Medical Research Council Laboratory for Molecular Cell Biology, University College London, Gower Street, London, WC1E 6BT, UK

²Institute for the Physics of Living Systems, University College London, London, United Kingdom

³College of Information and Control, Nanjing University of Information Science and Technology, Nanjing, Jiangsu 210044, China

Keywords: Intercalation, morphogenesis, fluidity, mechanics, vertex model

Summary

The ability of cells to exchange neighbours, termed intercalation, is a key feature of epithelial tissues. Intercalation is predominantly associated with tissue deformations that drive morphogenesis. More recently, however, intercalation that is not associated with large-scale tissue deformations has been described both during animal development and in mature epithelial tissues. This latter form of intercalation appears to contribute to an emerging phenomenon that we refer to as tissue fluidity – the ability of cells to exchange neighbours without changing the overall dimensions of the tissue. Here we discuss the contribution of junctional dynamics to intercalation governing both morphogenesis and tissue fluidity. In particular, we focus on the relative roles of junctional contractility and cell-cell adhesion as the driving forces behind intercalation. These two contributors to junctional mechanics can be used to simulate cellular intercalation in mechanical computational models, to test how junctional cell behaviours might regulate tissue fluidity and contribute to the maintenance of tissue integrity and the onset of disease.

Planar Cell Intercalation and the Role of Cell-Cell Junctions

Cell intercalation (here referred to purely as intercalation) is the process through which cells within an epithelium exchange neighbours (Figure 1a). While intercalation can occur perpendicular to the plane of an epithelium (termed radial intercalation), for instance when producing a stratified epithelium from a monolayered precursor, this review will focus exclusively on planar intercalation. Furthermore, although there are multiple mechanisms through which intercalation can occur (cell protrusive activity (1, 2), tissue stress (3-5)), we will focus on intercalation that is mediated by the dynamics of intercellular junctions. Specifically, we will discuss the contribution of adhesion at adherens junctions and contractility to intercalation. Adherens junctions are the predominant sites of intercellular adhesion (mainly through Cadherin homophilic adhesion molecules) and are coupled to the contractile cortical actomyosin cytoskeleton (6). Therefore, adherens junctions represent a region within the cell that both generates and integrates mechanical forces across cells and

*Author for correspondence (y.mao@ucl.ac.uk).

†Present address: Medical Research Council Laboratory for Molecular Cell Biology, University College London, Gower Street, London, WC1E 6BT, UK

1 tissues (7).

2 An emerging picture is that cell intercalation can act in two ways in a tissue. The first
3 is to deform a tissue, resulting in morphogenesis, which involves a change in the
4 dimensions of the tissue (Figure 1b). The second is to allow cells to exchange neighbours
5 without a change in the size or shape of the tissue (Figure 1c). In such a situation, cell
6 intercalations are analogous to the rearrangement of molecules in a fluid in a container that
7 does not change its dimensions. We therefore refer to this as “tissue fluidity”. A common
8 feature of these examples is that intercalation behaviours can be explained at the level of
9 cell-cell junctions. In this review, we aim to discuss how intercalation is regulated to achieve
10 these two functions and how computational modelling approaches can be used to
11 understand the mechanical basis of intercalation at the level of cell-cell junctions.

12 13 14 Intercalation Can Deform Developing Tissues

15
16 A conserved element of animal development is the extension of a tissue in one axis,
17 concomitant with a narrowing of the tissue in the orthogonal axis. This process is termed
18 convergent extension (or convergence and extension) and is driven by polarised
19 intercalation in many examples. The contribution of intercalation to convergent extension
20 can be clearly illustrated by two developmental morphogenetic processes - axis extension
21 and tubule elongation.

22 23 Axis Extension

24
25 Perhaps the most striking example of convergent extension in animal development is
26 the extension of the embryonic body axis (Figure 2a). Classically, embryos will extend along
27 their anteroposterior axis and converge along the orthogonal axis (referred to as
28 dorsoventral or mediolateral depending on the system).

29 Arguably, the most thoroughly studied example of axis extension is in the embryonic
30 germband in *Drosophila* (germband extension, GBE). As intercalation is a dynamic process,
31 it is best studied through live imaging and the simple epithelium of the germband in
32 *Drosophila* embryos is particularly well suited to this technique. It is likely that this is the
33 reason that the majority of our understanding of intercalation comes from work in
34 *Drosophila*, as is reflected in this review. During GBE, the germband extends roughly
35 twofold along its AP axis, while narrowing by the same magnitude along its DV axis (Figure
36 2a). This process is characterised by many polarised intercalation events (8), in which DV
37 oriented cell-cell junctions preferentially shrink and a new junction grows along the AP axis
38 (9).

39 GBE intercalation can take two forms. The first involves a tetrad of cells and is often
40 described as a “T1 process” using terminology from dynamics within foams (10). A DV
41 junction shared between two neighbouring cells (much like a wall shared between two
42 bubbles within a soap foam) initially shrinks to a single point, producing a 4-way junction in
43 which all four cells of the tetrad come into contact (Figure 2a). Subsequently, a new junction
44 grows along the AP axis, resulting in an exchange of neighbours within the tetrad (9). The
45 T1 mode of intercalation predominates early during GBE, but later, a second form of
46 intercalation is initiated. This involves the shrinkage of multiple connected DV-oriented
47 junctions shared by more than four cells, which ultimately produces a multicellular structure
48 known as a rosette (11). This rosette is then resolved along the AP axis, again resulting in
49 exchanges of neighbours (Figure 2a).

1 GBE intercalation has a mechanical basis, as it relies on the combined activity of the
2 contractile actomyosin cytoskeleton and intercellular adhesion. Cell surface mechanics
3 predicts that a contractile junction will shrink, while an adhesive junction will be prone to
4 grow (12). Indeed, there is a striking polarisation of both actin and myosin II in the
5 germband, which are both preferentially enriched at shrinking DV-oriented junctions in both
6 T1s (9, 13) and the multicellular cables generating rosettes (11, 14). Myosin II activity is
7 required for both active intercalation and axis extension (9). Moreover, myosin II and its
8 activity must be planar polarised, otherwise again both intercalation and axis extension fail
9 (11, 13, 15, 16). Furthermore, components of cell-cell adhesion complexes such as E-
10 Cadherin (E-Cad) and β -catenin are polarised in the opposite orientation (11). Interestingly,
11 planar polarised endocytosis of E-Cad is required to downregulate adhesion at DV-oriented
12 junctions (17). When endocytosis is blocked, intercalation fails almost entirely leading to a
13 drastic reduction in GBE. Therefore, increased contractility and decreased adhesion act in
14 concert to permit junction shrinkage (Figure 2b).

15 Polarised junctional myosin not only promotes junction shrinkage during *Drosophila*
16 GBE, but also drives intercalation in chordate systems undergoing axis extension. During
17 convergent extension of the chordate notochord, cells intercalate mediolaterally (18-20).
18 This process is most often described as being driven by polarised protrusive activity and
19 directed cell crawling (1, 2). However, more recently a role for polarised junction dynamics
20 has emerged in *Xenopus*. Phosphorylated myosin localises strongly to mediolaterally
21 oriented junctions in the notochord, which are also under increased tension, suggesting an
22 additional role for junction shrinkage in notochord convergent extension (21).

23 In chick embryos, myosin cables form perpendicular to the direction of primitive
24 streak formation and drive polarised junctional shrinkage (22). Similarly, mediolaterally
25 oriented actomyosin cables form in the neural plate of chick embryos. These are required
26 for shrinkage of mediolateral junctions, leading to the convergent extension of the neural
27 tube (23). Relatively little is understood about the contribution of junctional adhesion to axis
28 extension in vertebrate systems. There is some evidence that Cadherins play a role in
29 *Xenopus* axis extension (24, 25), however it will be interesting to see whether reciprocal
30 roles of contractility and adhesion are conserved.

31 Although myosin is strongly polarised at the level of cell-cell junctions, during GBE a
32 second pool of myosin also has a role in generating the forces required for DV junction
33 shrinkage. Myosin also localises in a medial pool, in the centre of cells, away from junctions.
34 During GBE, the medial pool of myosin coalesces into “pulses” that appear to flow into DV-
35 oriented junctions (Figure 2b) and these flows are temporally correlated with a reduction in
36 junction length (26). Interestingly it appears that these pulses are required to shorten the
37 junctions, while the pool of myosin tightly associated with the junctions stabilises this length
38 reduction (26), apparently through scission of Rab35 compartments and membrane removal
39 (27). The flows are dependent on planar polarised distributions of E-Cad (26), which display
40 transient asymmetries (due to E-Cad endocytosis) that permit the flow of myosin towards
41 regions of strongest anchoring of the actomyosin meshwork where E-Cad concentration is
42 highest (28).

43 Historically, the GBE field has been dominated by work focussing on apical cell
44 behaviours. However, cells are polarised along their apicobasal axes and more recently a
45 role for basal cell behaviours in GBE intercalation has emerged. In the majority of cases,
46 rosettes resolve basally first, suggesting basal dynamics are the main driving force of
47 intercalation. Basal cell protrusions are observed during GBE and when they are abolished,
48 many rosettes fail to resolve and GBE is reduced (29). However, when either basal
49 protrusions or myosin activity throughout the cell are abolished, a subset of rosettes still
50 resolve apically and basally (29) suggesting mechanical cooperativity between apical and
51 basal sides of the same cell.

1 So far we have focussed on the early stages of intercalation, when junctions
2 decrease in length to produce vertices shared by more than three cells. For cells to acquire
3 new neighbours, however, this multicellular vertex must be resolved to produce two or more
4 tricellular junctions (Figure 2a). This is achieved by the formation of a new cell-cell junction,
5 a process that like junction shrinkage, is dependent on actomyosin contractility. Unlike
6 junction shrinkage, new junction growth is a cell non-autonomous process driven by myosin
7 activity in the cells that were previously neighbours (30, 31) (Figure 2c). Pulses of
8 actomyosin, much like those contributing to junction shrinkage, form at regions within these
9 cells close to the newly formed tricellular junctions (32) and this is coupled with transient
10 contractions of apical cell area (30). The activity of myosin causes these cells to exert a
11 local pulling force on the new junction, which in turn is thought to promote junction
12 elongation, initially independently of E-Cad in the growing junctions (32). Local cell non-
13 autonomous forces are also required for junction elongation in the *Drosophila* amnioserosa
14 (33), suggesting that this may be a general mechanism of junction growth. In the germband,
15 an additional tissue scale pulling force from the invagination of the posterior midgut (32, 34)
16 aligns new junction growth along the AP axis (32).

17 For intercalation to be successful, there must therefore be tight spatiotemporal
18 regulation of junction shrinkage and new junction growth. If there is no temporal separation
19 between the two processes, they will antagonise each other (as a junction cannot both grow
20 and shrink at the same time) resulting in a failure of cell intercalation. Evidence that this is
21 true comes from work performed in the pupal wing of *Drosophila*. The pupal wing displays
22 significant intercalation when undergoing morphogenesis to produce the shape of the adult
23 wing blade (3, 35). Timely removal of myosin II (and its activator Rho kinase (Rok)) from
24 new junctions is crucial to allow multicellular vertices to resolve and for these new junctions
25 to grow (31). Myosin II removal from new junctions in the pupal wing is controlled by
26 Phosphatase and tensin homologue (PTEN), which drives the conversion of PIP3 to PIP2
27 (36). When this pathway is disrupted, myosin II remains concentrated in the new junctions
28 and cells fluctuate back and forth through four-way vertices. Therefore, it appears that
29 dissipation of tension in growing junctions is required for their growth (Figure 2c), which was
30 supported by computational modelling of pupal wings (31). The same is likely to be true
31 during GBE, as when a constitutively active, phosphomimetic form of myosin regulatory
32 light chain (MRLC) is expressed in place of wildtype MRLC, there is an increase in the
33 number of junctions that fail to resolve correctly (16).

34 35 Tubule Elongation

36
37 While axis extension is a key process driven by convergent extension, there are
38 other developmental processes which require the simultaneous elongation and narrowing of
39 a tissue. Tubule elongation is one such example where intercalation can contribute to
40 organogenesis.

41 Tubule elongation can involve oriented growth and cell shape changes among other
42 mechanisms, however, often the process instead relies on the rearrangement of cells (37).
43 Again, much work has been performed on the role of intercalations in tubule elongation in
44 *Drosophila* embryos, particularly in the Malpighian Tubules (which form the fly's renal
45 system) and tracheal network (which is the site of gaseous exchange). The Malpighian
46 Tubule lumen is initially lined by up to twelve cells when viewed in cross section (38).
47 However, at later stages of development, only two cells contact the lumen in cross section,
48 which is achieved by cells intercalating between each other in the circumferential axis
49 (Figure 2a). This reduction in luminal cell number is associated with a vast proximodistal
50 elongation and concomitant circumferential convergence. Circumferential intercalation in the
51 tubule is, as in *Drosophila* GBE, driven by polarised pulses of myosin II. However, unlike

1 during GBE, these pulses are localised to the basal surface of the tubule cells (38).
2 Intercalation in the Malpighian Tubules is therefore cell autonomous, as evidenced by
3 intercalation and extension of Malpighian Tubules cultured externally to the embryo (39).
4 This is in contrast to intercalation in the tracheal network, which is a cell non-autonomous
5 process (40). In the developing dorsal branches of the tracheal network, the distal most
6 cells (known as tip cells) mechanically pull on the tubules to generate a proximodistally
7 oriented force. Intercalation in the tracheal branches can be entirely suppressed by ablation
8 of the leading tip cell.

9 Interestingly, intercalation in the trachea still relies on junction dynamics to some
10 extent, but in terms of adhesion (41) rather than actomyosin based contractility (42).
11 Intercalation can be suppressed genetically in the trachea (43) and this appears to be due to
12 a reduction in E-Cad turnover. It is thought that this may render junctions fixed in one
13 confirmation, unable to remodel to allow intercalation to proceed (41). Despite a lack of
14 intercalation in this situation, trachea are still able to elongate to a large extent (40).
15 Therefore, elongation drives intercalation, rather than the reverse being true as in GBE.

16 Cell intercalation in tubule elongation is not a peculiarity of *Drosophila*, as similar
17 observations have been made during vertebrate tubulogenesis. In the developing renal tube
18 of *Xenopus*, rosette-based intercalations are prevalent and associated with tubule
19 elongation (44). Furthermore, both elongation and rosette formation are dependent on
20 polarised distributions of myosin II, arguing that cell rearrangements are vital for elongation.
21 Multicellular rosettes can also be found in developing mouse kidney collecting ducts (44)
22 and cochlea (45), suggesting that this mechanism of tubule elongation may be conserved
23 throughout vertebrates.

24 25 26 Intercalation Without Tissue-Level Deformation

27
28 It is clear from the examples above that cell intercalation has the capacity to drive
29 tissue morphogenesis. More recently, however, evidence has emerged that intercalation
30 can equally be associated with tissues that are comparably static in nature. In these
31 examples, although cells exchange neighbours, the overall boundaries, and therefore the
32 shape of the tissue, remain unchanged. As we describe earlier, we term this phenomenon
33 “tissue fluidity”.

34 35 36 Non-morphogenetic Intercalation in the *Drosophila* Notum

37
38 The pupal notum of *Drosophila* is an example of a tissue undergoing intercalation
39 events that do not contribute to tissue deformation (Figure 3). In this tissue, although
40 intercalations are frequent, the tissue itself does not undergo any overall deformation (46).
41 In other words, its overall boundary conditions do not change significantly. Instead of highly
42 deterministic changes in junction length, intercalations appear to occur as a consequence of
43 stochastic fluctuations in junction length. Long junctions can shrink and grow without
44 inducing an intercalation event. However, when a short junction shrinks completely the
45 resulting four-way vertex can sometimes resolve in the orthogonal direction, leading to an
46 exchange of neighbours. The non-deterministic nature of these intercalations is particularly
47 highlighted by a subset of intercalations which only result in a transient neighbour
48 exchange, something that appears to be shared by the larval wing imaginal disc of
49 *Drosophila* (47).

1 The non-deterministic nature of intercalations not only applies to the length of
2 junction changes, but also to the orientation of these changes. Surprisingly, given what is
3 known about intercalation in the systems described above, notum intercalations are not
4 polarised and are not driven by highly polarised distributions of actomyosin. Instead these
5 intercalations occur due to stochastic variations in junctional myosin levels, which occur in
6 random orientations. The importance of fluctuations in myosin have been demonstrated
7 through computational modelling (46) (see section below).

8 As well as being controlled by local stochastic fluctuations in myosin concentration,
9 the rate of intercalation in the notum is controlled by the global average level of junctional
10 tension (46). Early in notum development, myosin concentration and junctional tension are
11 low, which is associated with a high intercalation rate. Later in development, the
12 concentration of myosin and junctional tension are much higher and this correlates with a
13 reduction in the rate of intercalation. The notion that myosin contractility might in fact be
14 inhibitory to cell intercalation in the notum was confirmed by genetically perturbing myosin
15 activity throughout the notum. Hyperactivation of myosin led to a decrease in intercalation,
16 while inactivation of myosin increased the rate of intercalation (Figure 3). The increase in
17 junctional tension over time, and the corresponding decrease in intercalation rate, is
18 associated with a gradual improvement in cell packing (46). As tension gradually increases,
19 so too does the proportion of hexagonal cells (also verified by computation modelling, see
20 later), suggesting that the regulation of tissue fluidity in the notum has a role in tissue
21 patterning.

22 The role of myosin II in intercalation in *Drosophila* therefore appears to be highly
23 context dependent. In polarised systems such as the germband and Malpighian tubule,
24 myosin II directs the selective shortening of junctions along a single axis. In an unpolarised
25 system, global tissue properties dominate, however this must be coupled with fluctuations in
26 Myosin activity.

27 The gradual decrease of tissue fluidity in the notum is reminiscent of an epithelial
28 fluid-to-solid jamming transition (48, 49). Jamming terminology is derived from the physics
29 of particulate matter where a fluid-to-solid jamming transition occurs when particles can no
30 longer move past each other due to increased density (50). In a cell layer a fluid-to-solid
31 jamming transition occurs when cells can no longer exchange neighbours through
32 intercalation. The latter is distinct from jamming in particulate matter, as it is independent of
33 the density of cells (48). The theory that explains unjamming, which sheds light on tissue
34 fluidity in certain contexts, will be explored in the following sections

35 36 Tissue Fluidity and Disease

37
38 The epithelial jamming transition has been recently implicated in disease; specifically,
39 asthma. Cultured monolayers of differentiated human bronchial epithelial cells (HBECs)
40 undergo a transition from a solid-like jammed phase to a fluid-like unjammed phase when
41 subjected to an apicobasal compression of a magnitude that mimics that encountered
42 during asthmatic bronchospasm (49). Furthermore, during HBEC layer maturation after
43 reaching confluency, a fluid-to-solid jamming transition is observed. Cell fluidity is high on
44 early culture days but decreases with age of the culture, until the cell monolayer is almost
45 completely static. This may be a general property of maturing epithelial cell layers, as
46 recently the same has been observed in epidermal progenitor cell (EPC) monolayers (51). It
47 is unclear what drives this jamming transition during maturation at the cellular level,
48 however it is likely to be related to cell-cell adhesion and cortical contractility (and this will
49 be explored in the following section).

50 Intriguingly, the fluid-to-solid jamming transition is delayed in monolayers of HBECs
51 derived from asthmatic donors. What the functional significance of this is remains to be

1 seen, however it suggests that hyperfluidity of epithelial layers might contribute to
2 pathogenesis. Furthermore, it remains to be tested whether HBEC layers derived from
3 asthmatic patients respond in the same way to compression.

4 Like in the *Drosophila* notum, the induced fluidity does not contribute to changes in
5 the dimension of the cell layer. For HBEC layers, the confines of the culture dish provide a
6 clear physical boundary to the cell layer that cannot be deformed. This then raises the
7 question of whether static boundaries (meaning the tissue does not change size or shape)
8 contribute to fluidity or whether the stochastic nature of intercalations maintains the
9 boundary's dimensions. This is challenging to test, as by removing a boundary you create a
10 free edge in the cell layer which is likely to induce effects independent of intercalation, such
11 as an increase of boundary contractility (52). One possible method that could be used to
12 explore this question is computational modelling, which will be discussed in the following
13 section.

14 This potential contribution of unregulated tissue fluidity to disease is to our
15 knowledge a first. With the advent of more physiological culturing systems such as lung-on-
16 a-chip (53) and organoid technology (54), both amenable to live cell imaging, it will be
17 fascinating to see if tissue fluidity might relate to underlying causes of other epithelial
18 diseases.

19 20 Why Do Tissues Regulate Their Fluidity?

21
22 In the *Drosophila* notum, it appears that the regulation of tissue fluidity is connected
23 to the preservation of cell shape, patterning and packing. As junctional tension increases
24 through development, the notum becomes increasingly hexagonally packed (Figure 3) (46).
25 Another striking example of tissue fluidity is that of the chick epiblast (55). During
26 gastrulation, many intercalation events occur, which are associated with cell divisions.
27 Epiblast fluidity shares parallels with the *Drosophila* notum, as reduced cortical tension
28 facilitates cell division-mediated intercalation (55). Fluidity in the epiblast appears to have a
29 clear role in patterning gastrulation movements, possibly by relaxing forces generated by
30 cell behaviours in the neighbouring primitive streak. When fluidity is inhibited by blocking
31 cell division (and subsequently the majority of intercalations) the characteristic "Polonaise
32 movements" of chick gastrulation are strongly disrupted (55). However, why the bronchial
33 airway epithelium should undergo an unjamming transition in response to compression
34 remains unclear. Future work investigating the fluidity of other tissues in contexts such as
35 development and tissue homeostasis will hopefully begin to shed more light on the function
36 of tissue fluidity. On the other hand, the regulation of tissue fluidity during cell layer
37 maturation raises the intriguing possibility, that the ability of a mature tissue to be fluid under
38 certain conditions might be linked to tissue robustness. A specific example is after tissue
39 wounding. Tissues may need to fluidise after injury, explore new configurations, then
40 resettle into a new solid like state.

41 When an epithelial tissue is wounded, a gap is created that the existing cells need to
42 fill. One possible way cells could "flow" into this gap is to rearrange relative to each other in
43 a directional manner, similar to intercalation during convergent extension. Such an
44 observation has been made in the *Drosophila* embryonic ectoderm. Here, the strategy for
45 intercalation during germband extension appears to be "redeployed" to allow these epithelial
46 wounds to close (56). Cells a few rows from an ectodermal wound edge undergo
47 intercalation events driven by pulsatile flows of myosin that are qualitatively identical to
48 those seen during GBE. The role of these intercalations appears to be to allow the wound
49 edge to move forwards, as when intercalation is inhibited by reducing myosin activity,
50 wound healing is slower (56). Strictly speaking, while these wounds are healing and cells
51 are intercalating, the outer boundaries of the ectoderm do not change. Therefore, this

1 represents an example where tissue fluidity is driven by polarised localisations of myosin.
2 Interestingly, this is reminiscent of another situation where a polarised tissue is challenged
3 by introducing new static boundaries in the germband (32). With static boundaries, the
4 tissue can no longer extend along the AP axis, however the rate of cell intercalation is
5 unchanged and cells readily exchange neighbours (32), meaning that the tissue has
6 become fluid by the terms of our definition of tissue fluidity. Therefore, it appears that the
7 presence of unchanging tissue boundaries can induce tissue fluidity even in situations
8 where intercalation is polarised.

9 It will be interesting to see whether actively driven polarised intercalation events,
10 when combined with fixed tissue boundaries, have a role in driving fluidity in other contexts.
11 In particular, it remains to be seen whether polarised intercalation is used to induce fluidity
12 during wound closure in more mature epithelia (and not just embryos), or whether stochastic
13 junctional fluctuation-induced tissue fluidity might have a role. Certainly, there are other
14 indications that tissue fluidity might contribute to wound closure. Maturation of a cultured cell
15 monolayer shares parallels with wound closure, in that a functional barrier needs to be
16 formed during the process. It is fascinating that asthmatic patients have impaired wound
17 healing in the lung (57) and that asthmatic HBEC monolayers are fluid for longer during
18 maturation (49). One might hypothesise that if an unjamming or jamming transition is
19 delayed, this might be connected to failures in wound healing. However, this remains to be
20 tested.

21 Adhesions also play a role in wound closure. Eph-ephrin signalling is upregulated in
22 wounded mouse and human skin and this is required to downregulate cell-cell adhesion at
23 tight junctions and adherens junctions (58). In keratinocyte culture scratch wound assays,
24 removal of Eph-ephrin signalling reduces the ability of cells to move into the wound,
25 although it is unclear whether this is due to increased migration or through increased
26 intercalation. However, increased Eph-ephrin signalling appears to downregulate tension in
27 cells surrounding the wound by dissolving actomyosin stress fibres (58), which is consistent
28 with the notion that decreased epithelial tension is associated with increased tissue fluidity.
29 On the other hand, hyperactivation of Eph-ephrin signalling in wounded skin appears to lead
30 to defective healing as a result of an almost total loss of adhesion between cells (58). This
31 highlights that a delicate balance between cell cohesiveness and fluidity is likely key for
32 intercalation mediated events, both in development and disease.

33 34 35 Understanding Intercalation using Vertex-Based Models

36
37 Above, we have described examples of experimental work that has furthered our
38 understanding of intercalation in many contexts. However, dissecting the relative roles of
39 tissue mechanics and biochemical signalling experimentally remains challenging. For this
40 reason, the field is increasingly turning to computational models to understand how
41 intercalation contributes to morphogenesis and how the mechanical properties of a tissue
42 can contribute to fluidity.

43 While a number of models exist (for instance the Cellular Potts (59), “cell-centre” (60)
44 and “finite-element” (61) models), vertex-based models have arguably increased our
45 understanding of intercalation the most. Vertex models (62) describe a layer of epithelial
46 cells as a network of vertices (which represent tricellular junctions and vertices at the centre
47 of higher order structures, such as rosettes) connected by junctions (representing bicellular
48 junctions) (Figure 4a). Vertex modelling of an epithelium relies on the relationship between
49 three key properties of cells that determine the movement of vertices; cell area elasticity,
50 cell perimeter contractility and the line tension of individual junctions (described in detail in

1 Figure 4d). In combination, these define an energy function that the model aims to minimise
2 (Figure 4b) (62).

3 Vertex modelling has been used to understand how intercalation contributes to
4 convergent extension during GBE in more detail. Key to modelling GBE is to use the line
5 tension term to introduce polarity into the simulated system. In such models, intercalation
6 events occur when junctions shorten to a threshold length and are then allowed to resolve
7 orthogonally, provided this reduces the energy in the model (63-65) (Figure 4c). Taking this
8 approach, vertex modelling has demonstrated that intercalation driven by polarised
9 junctional tension can explain the convergent extension of 2D fields of cells (63), 3D
10 aggregates and tubes (65). Interestingly, modelling suggests that polarised junction
11 contraction only allows tissues to extend up to roughly 2.5 times their original length (65).
12 This may indicate that there is an inherent property of the germband that prevents it from
13 attempting to extend continuously.

14 A further vertex model of GBE was used to investigate the interaction between
15 patterning of the germband and intercalation (64). The germband is patterned along its AP
16 axis by a hierarchical cascade of spatially restricted genes into discrete domains (66).
17 These “AP patterning genes” are required to polarise myosin activity to DV-oriented
18 junctions (8, 13) at the boundaries of domains through local cell-cell interactions (64)
19 mediated by Toll receptors (67). In the model, line tension was increased at boundaries
20 between spatial domains, to mimic myosin polarisation. Myosin concentration increases at
21 junctions as they shrink during GBE, therefore length dependency was introduced to the line
22 tension term in the model. This model demonstrated that myosin polarity, like those above,
23 could drive convergent extension of the germband. However, it also predicted that
24 restricting myosin contractility to junctions between AP spatial domains was sufficient to
25 maintain the order of these predefined AP domains along the body axis (64).

26 The above examples demonstrate that intercalation can be successfully modelled by
27 introducing polarised contractility into vertex models to explain morphogenesis and the
28 maintenance of tissue order. However, vertex models have hugely furthered our
29 understanding of how tissue mechanics might contribute to tissue fluidity in the context of
30 tissue unjamming. Again, fluidity through unjamming can be explained theoretically by the
31 mechanical properties of cell-cell junctions. Vertex modelling has been particularly useful to
32 explain the transition from a jammed, immobile epithelium to an unjammed, fluid epithelium.

33 In contrast to modelling polarised intercalation, when modelling intercalations
34 associated with tissue unjamming, vertex model parameters do not vary across cells or
35 between junctions. The relative contributions of perimeter contractility (determined by the
36 sum of perimeter contractility and cell-cell junction line tension) and cell area interact to give
37 cells a preferred cell shape. This can be described by a cell shape parameter (ρ_0) which is
38 the ratio between the preferred perimeter and square root of the preferred area ($\rho_0 = P/\sqrt{A}$)
39 (48). Therefore, the energy function of the vertex model can be phrased in terms of how far
40 a cell's shape deviates from its preferred shape. Inherently, cells must change shape to
41 allow an exchange of neighbours. Thus, the magnitude of the energy cost of cell shape
42 changes (specifically how easily a cell can deviate from its preferred shape) determines how
43 easily cells can intercalate (49). This energy barrier is determined by ρ_0 itself and as ρ_0
44 increases, the energy barrier decreases. When ρ_0 reaches a threshold value of 3.81, the
45 energy barrier to cell shape changes becomes vanishingly small (48) meaning that such a
46 system can readily undergo intercalation and therefore is in a fluid regime. Accordingly, the
47 shear modulus vanishes at this transitional ρ_0 value (48).

48 This apparent link between cell shape and fluidity has been probed using the HBEC
49 monolayers described earlier. When ρ_0 in jammed and unjammed HBEC monolayers was
50 quantified, it was on average closer to the theoretical threshold value of 3.81 in unjammed

1 layers than jammed layers (49). This therefore supports the notion that the increased ability
2 of cells to change shape promotes tissue fluidity.

3 One failing of this model is that it does not describe a dynamic epithelium, but
4 instead reaches steady state and infers fluidity from cell shape. Therefore, intercalation rate,
5 *per se*, cannot be quantified from the model. Vertex modelling of the *Drosophila* notum
6 introduced dynamics by having an additional term describing stochastic fluctuations in edge
7 tension (46). In this model, edge tension fluctuations are derived from spatiotemporal
8 quantification of myosin intensity from live imaging. This approach was able to recapitulate
9 the fluidity of the notum. Moreover, increasing the average magnitude of line tension in this
10 model was sufficient to increase the proportion of hexagonal cells in simulations. This was
11 also observed in the more mature notum and is a hallmark of a jammed epithelium
12 undergoing fewer intercalations (Figure 3) (46).

13 Based on data from the *Drosophila* notum vertex model, it is possible that non-
14 deterministic fluctuations in cell edge tension (either through changes in contractility or
15 adhesion) also contribute to the fluidity of HBEC monolayers in the same manner as the
16 *Drosophila* notum. However, to confirm this, quantitative analysis of myosin and cell-cell
17 adhesion must be performed in HBEC layers.

18 19 20 Conclusion

21
22 In this review we have discussed the contribution of intercalation to morphogenesis
23 and tissue fluidity. The key difference between these two functions appears to be
24 associated with whether the tissue undergoes a deformation or not. Much is understood
25 about the role of intercalation in morphogenesis and how it is driven by a combination of
26 regulated cortical contractility and cell-cell adhesion. Comparatively little is known about
27 intercalation in tissue fluidity. However, it appears that it can similarly be explained by the
28 properties of cell-cell junctions. The regulation of tissue fluidity may have more far reaching
29 consequences, as it appears that the induction of a jammed state is important for both
30 inducing cell differentiation and delamination from the embryonic mouse epidermis, to drive
31 stratification (51). It will be fascinating to understand in more detail how tissue fluidity
32 contributes to development, homeostasis and disease.

33 34 35 Additional Information

36 **Acknowledgments**

37 Thank you to members of the Mao group for giving feedback on the manuscript.

38 39 **Authors' Contributions**

40 RJT and YM conceived and wrote the article.

41 42 **Competing Interests**

43 We have no competing interests.

44 45 **Funding**

46 RJT is funded by a Medical Research Council Skills Development Fellowship (MR/N014529/1). YM is funded by a
47 Medical Research Council Fellowship MR/L009056/1, a UCL Excellence Fellowship, and a NSFC International Young
48 Scientist Fellowship 31650110472. This work was also supported by MRC funding to the MRC LMCB University Unit at
49 UCL, award code MC_U12266B.

1 References

1. Shi W, Peyrot SM, Munro E, Levine M. FGF3 in the floor plate directs notochord convergent extension in the *Xenopus* tadpole. *Development*. 2009;136(1):23-8.
2. Shih J, Keller R. Cell motility driving mediolateral intercalation in explants of *Xenopus laevis*. *Development*. 1992;116(4):901-14.
3. Aigouy B, Farhadifar R, Staple DB, Sagner A, Roper JC, Julicher F, et al. Cell flow reorients the axis of planar polarity in the wing epithelium of *Drosophila*. *Cell*. 2010;142(5):773-86.
4. Lau K, Tao H, Liu H, Wen J, Sturgeon K, Sorfazlian N, et al. Anisotropic stress orients remodelling of mammalian limb bud ectoderm. *Nat Cell Biol*. 2015;17(5):569-79.
5. Wen J, Tao H, Lau K, Liu H, Simmons CA, Sun Y, et al. Cell and Tissue Scale Forces Coregulate Fgfr2-Dependent Tetrads and Rosettes in the Mouse Embryo. *Biophys J*. 2017;112(10):2209-18.
6. Lecuit T, Yap AS. E-cadherin junctions as active mechanical integrators in tissue dynamics. *Nature Cell Biology*. 2015;17(5):533-9.
7. Lecuit T, Lenne PF, Munro E. Force generation, transmission, and integration during cell and tissue morphogenesis. *Annu Rev Cell Dev Biol*. 2011;27:157-84.
8. Irvine KD, Wieschaus E. Cell intercalation during *Drosophila* germband extension and its regulation by pair-rule segmentation genes. *Development*. 1994;120(4):827-41.
9. Bertet C, Sulak L, Lecuit T. Myosin-dependent junction remodelling controls planar cell intercalation and axis elongation. *Nature*. 2004;429(6992):667-71.
10. Cox SJ, Vaz MF, Weaire D. Topological changes in a two-dimensional foam cluster. *Eur Phys J E*. 2003;11(1):29-35.
11. Blankenship JT, Backovic ST, Sanny JS, Weitz O, Zallen JA. Multicellular rosette formation links planar cell polarity to tissue morphogenesis. *Dev Cell*. 2006;11(4):459-70.
12. Lecuit T, Lenne PF. Cell surface mechanics and the control of cell shape, tissue patterns and morphogenesis. *Nat Rev Mol Cell Biol*. 2007;8(8):633-44.
13. Zallen JA, Wieschaus E. Patterned gene expression directs bipolar planar polarity in *Drosophila*. *Dev Cell*. 2004;6(3):343-55.
14. Fernandez-Gonzalez R, Simoes Sde M, Roper JC, Eaton S, Zallen JA. Myosin II dynamics are regulated by tension in intercalating cells. *Dev Cell*. 2009;17(5):736-43.
15. Simoes Sde M, Blankenship JT, Weitz O, Farrell DL, Tamada M, Fernandez-Gonzalez R, et al. Rho-kinase directs Bazooka/Par-3 planar polarity during *Drosophila* axis elongation. *Dev Cell*. 2010;19(3):377-88.
16. Kasza KE, Farrell DL, Zallen JA. Spatiotemporal control of epithelial remodeling by regulated myosin phosphorylation. *Proc Natl Acad Sci U S A*. 2014;111(32):11732-7.
17. Levayer R, Pelissier-Monier A, Lecuit T. Spatial regulation of Dia and Myosin-II by RhoGEF2 controls initiation of E-cadherin endocytosis during epithelial morphogenesis. *Nat Cell Biol*. 2011;13(5):529-40.
18. Keller R, Tibbetts P. Mediolateral cell intercalation in the dorsal, axial mesoderm of *Xenopus laevis*. *Dev Biol*. 1989;131(2):539-49.
19. Keller RE, Danilchik M, Gimlich R, Shih J. The function and mechanism of convergent extension during gastrulation of *Xenopus laevis*. *J Embryol Exp Morphol*. 1985;89 Suppl:185-209.
20. Jiang D, Smith WC. Ascidian notochord morphogenesis. *Dev Dyn*. 2007;236(7):1748-57.
21. Shindo A, Wallingford JB. PCP and septins compartmentalize cortical actomyosin to direct collective cell movement. *Science*. 2014;343(6171):649-52.
22. Rozbicki E, Chuai M, Karjalainen AI, Song F, Sang HM, Martin R, et al. Myosin-II-mediated cell shape changes and cell intercalation contribute to primitive streak formation. *Nat Cell Biol*. 2015;17(4):397-408.
23. Nishimura T, Honda H, Takeichi M. Planar cell polarity links axes of spatial dynamics in neural-tube closure. *Cell*. 2012;149(5):1084-97.
24. Marsden M, DeSimone DW. Integrin-ECM interactions regulate cadherin-dependent cell adhesion and are required for convergent extension in *Xenopus*. *Curr Biol*. 2003;13(14):1182-91.
25. Zhong Y, Briehner WM, Gumbiner BM. Analysis of C-cadherin regulation during tissue morphogenesis with an activating antibody. *J Cell Biol*. 1999;144(2):351-9.

26. Rauzi M, Lenne PF, Lecuit T. Planar polarized actomyosin contractile flows control epithelial junction remodelling. *Nature*. 2010;468(7327):1110-4.
27. Jewett CE, Vanderleest TE, Miao H, Xie Y, Madhu R, Loerke D, et al. Planar polarized Rab35 functions as an oscillatory ratchet during cell intercalation in the *Drosophila* epithelium. *Nat Commun*. 2017;8.
28. Levayer R, Lecuit T. Oscillation and polarity of E-cadherin asymmetries control actomyosin flow patterns during morphogenesis. *Dev Cell*. 2013;26(2):162-75.
29. Sun Z, Amourda C, Shagirov M, Hara Y, Saunders TE, Toyama Y. Basolateral protrusion and apical contraction cooperatively drive *Drosophila* germ-band extension. *Nat Cell Biol*. 2017;19(4):375-83.
30. Yu JC, Fernandez-Gonzalez R. Local mechanical forces promote polarized junctional assembly and axis elongation in *Drosophila*. *Elife*. 2016;5.
31. Bardet PL, Guirao B, Paoletti C, Serman F, Leopold V, Bosveld F, et al. PTEN controls junction lengthening and stability during cell rearrangement in epithelial tissue. *Dev Cell*. 2013;25(5):534-46.
32. Collinet C, Rauzi M, Lenne PF, Lecuit T. Local and tissue-scale forces drive oriented junction growth during tissue extension. *Nat Cell Biol*. 2015;17(10):1247-58.
33. Hara Y, Shagirov M, Toyama Y. Cell Boundary Elongation by Non-autonomous Contractility in Cell Oscillation. *Curr Biol*. 2016;26(17):2388-96.
34. Lye CM, Blanchard GB, Naylor HW, Muresan L, Huisken J, Adams RJ, et al. Mechanical Coupling between Endoderm Invagination and Axis Extension in *Drosophila*. *Plos Biology*. 2015;13(11).
35. Etournay R, Popovic M, Merkel M, Nandi A, Blasse C, Aigouy B, et al. Interplay of cell dynamics and epithelial tension during morphogenesis of the *Drosophila* pupal wing. *Elife*. 2015;4:e07090.
36. Maehama T, Dixon JE. The tumor suppressor, PTEN/MMAC1, dephosphorylates the lipid second messenger, phosphatidylinositol 3,4,5-trisphosphate. *J Biol Chem*. 1998;273(22):13375-8.
37. Andrew DJ, Ewald AJ. Morphogenesis of epithelial tubes: Insights into tube formation, elongation, and elaboration. *Dev Biol*. 2010;341(1):34-55.
38. Saxena A, Denholm B, Bunt S, Bischoff M, VijayRaghavan K, Skaer H. Epidermal growth factor signalling controls myosin II planar polarity to orchestrate convergent extension movements during *Drosophila* tubulogenesis. *PLoS Biol*. 2014;12(12):e1002013.
39. Broadie K, Skaer H, Bate M. Whole-embryo culture of *Drosophila* : development of embryonic tissues in vitro. *Roux Arch Dev Biol*. 1992;201(6):364-75.
40. Caussinus E, Colombelli J, Affolter M. Tip-cell migration controls stalk-cell intercalation during *Drosophila* tracheal tube elongation. *Curr Biol*. 2008;18(22):1727-34.
41. Shaye DD, Casanova J, Llimargas M. Modulation of intracellular trafficking regulates cell intercalation in the *Drosophila* trachea. *Nat Cell Biol*. 2008;10(8):964-70.
42. Ochoa-Espinosa A, Harmansa S, Caussinus E, Affolter M. Myosin II is not required for *Drosophila* tracheal branch elongation and cell intercalation. *Development*. 2017;144(16):2961-8.
43. Ribeiro C, Neumann M, Affolter M. Genetic control of cell intercalation during tracheal morphogenesis in *Drosophila*. *Curr Biol*. 2004;14(24):2197-207.
44. Lienkamp SS, Liu K, Karner CM, Carroll TJ, Ronneberger O, Wallingford JB, et al. Vertebrate kidney tubules elongate using a planar cell polarity-dependent, rosette-based mechanism of convergent extension. *Nat Genet*. 2012;44(12):1382-7.
45. Chacon-Heszele MF, Ren D, Reynolds AB, Chi F, Chen P. Regulation of cochlear convergent extension by the vertebrate planar cell polarity pathway is dependent on p120-catenin. *Development*. 2012;139(5):968-78.
46. Curran S, Strandkvist C, Bathmann J, de Gennes M, Kabla A, Salbreux G, et al. Myosin II Controls Junction Fluctuations to Guide Epithelial Tissue Ordering. *Dev Cell*. 2017;43(4):480-92 e6.
47. Heller E, Kumar KV, Grill SW, Fuchs E. Forces generated by cell intercalation tow epidermal sheets in mammalian tissue morphogenesis. *Dev Cell*. 2014;28(6):617-32.
48. Bi DP, Lopez JH, Schwarz JM, Manning ML. A density-independent rigidity transition in biological tissues. *Nat Phys*. 2015;11(12):1074-+.
49. Park JA, Kim JH, Bi D, Mitchel JA, Qazvini NT, Tantisira K, et al. Unjamming and cell shape in the asthmatic airway epithelium. *Nat Mater*. 2015;14(10):1040-8.
50. Biroli G. Jamming - A new kind of phase transition? *Nat Phys*. 2007;3(4):222-3.

51. Miroshnikova YA, Le HQ, Schneider D, Thalheim T, Rubsam M, Bremicker N, et al. Adhesion forces and cortical tension couple cell proliferation and differentiation to drive epidermal stratification. *Nat Cell Biol.* 2018;20(1):69-80.
52. Maitre JL, Berthoumieux H, Krens SFG, Salbreux G, Julicher F, Paluch E, et al. Adhesion Functions in Cell Sorting by Mechanically Coupling the Cortices of Adhering Cells. *Science.* 2012;338(6104):253-6.
53. Huh D, Matthews BD, Mammoto A, Montoya-Zavala M, Hsin HY, Ingber DE. Reconstituting organ-level lung functions on a chip. *Science.* 2010;328(5986):1662-8.
54. Barkauskas CE, Chung MI, Fioret B, Gao X, Katsura H, Hogan BL. Lung organoids: current uses and future promise. *Development.* 2017;144(6):986-97.
55. Firmino J, Rocancourt D, Saadaoui M, Moreau C, Gros J. Cell Division Drives Epithelial Cell Rearrangements during Gastrulation in Chick. *Developmental Cell.* 2016;36(3):249-61.
56. Razzell W, Wood W, Martin P. Recapitulation of morphogenetic cell shape changes enables wound re-epithelialisation. *Development.* 2014;141(9):1814-20.
57. Holgate ST, Davies DE, Lackie PM, Wilson SJ, Puddicombe SM, Lordan JL. Epithelial-mesenchymal interactions in the pathogenesis of asthma. *J Allergy Clin Immun.* 2000;105(2):193-204.
58. Nunan R, Campbell J, Mori R, Pitulescu ME, Jiang WG, Harding KG, et al. Ephrin-Bs Drive Junctional Downregulation and Actin Stress Fiber Disassembly to Enable Wound Re-epithelialization. *Cell Rep.* 2015;13(7):1380-95.
59. Graner F, Glazier JA. Simulation of Biological Cell Sorting Using a 2-Dimensional Extended Potts-Model. *Phys Rev Lett.* 1992;69(13):2013-6.
60. Pathmanathan P, Cooper J, Fletcher A, Mirams G, Murray P, Osborne J, et al. A computational study of discrete mechanical tissue models. *Phys Biol.* 2009;6(3).
61. Chen HH, Brodland GW. Cell-level finite element studies of viscous cells in planar aggregates. *J Biomech Eng-T Asme.* 2000;122(4):394-401.
62. Farhadifar R, Roper JC, Algouy B, Eaton S, Julicher F. The influence of cell mechanics, cell-cell interactions, and proliferation on epithelial packing. *Current Biology.* 2007;17(24):2095-104.
63. Rauzi M, Verant P, Lecuit T, Lenne PF. Nature and anisotropy of cortical forces orienting *Drosophila* tissue morphogenesis. *Nature Cell Biology.* 2008;10(12):1401-U57.
64. Tetley RJ, Blanchard GB, Fletcher AG, Adams RJ, Sanson B. Unipolar distributions of junctional Myosin II identify cell stripe boundaries that drive cell intercalation throughout *Drosophila* axis extension. *Elife.* 2016;5.
65. Honda H, Nagai T, Tanemura M. Two different mechanisms of planar cell intercalation leading to tissue elongation. *Dev Dynam.* 2008;237(7):1826-36.
66. Sanson B. Generating patterns from fields of cells - Examples from *Drosophila* segmentation. *Embo Rep.* 2001;2(12):1083-8.
67. Pare AC, Vichas A, Fincher CT, Mirman Z, Farrell DL, Mainieri A, et al. A positional Toll receptor code directs convergent extension in *Drosophila*. *Nature.* 2014;515(7528):523-7.

Figure and table captions

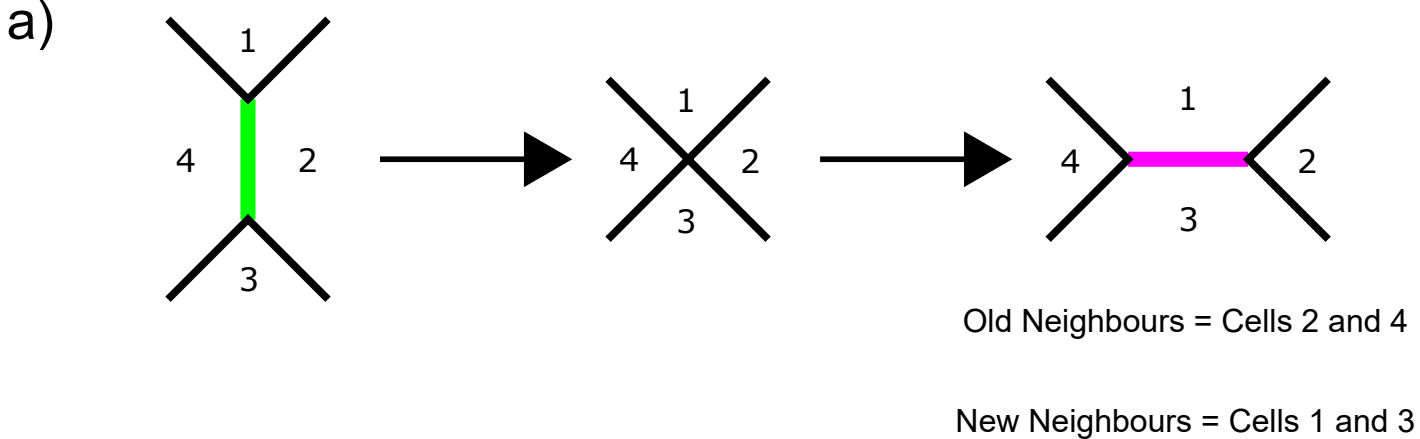
Figure 1. Cell intercalation is associated both with tissue deformation and with tissues having static boundaries. (a) During an intercalation event, a junction shared between two cells (green) shrinks to a single point creating a four-way vertex. This vertex then resolves in the orthogonal direction as a new junction (magenta) grows. This results in an exchange of neighbours. In a tissue, there are often multiple intercalation events associated with either (b) tissue deformation or (c) no tissue deformation (old shrinking and new growing junctions are coloured as in (a)). We refer to the latter example (c) as “tissue fluidity”.

Figure 2. Polarised intercalation deforms tissues during morphogenesis. (a) Morphogenesis, particularly examples of convergent extension such as axis extension (here shown *Drosophila* GBE, germband in grey, direction of elongation shown by red arrow) and tubule elongation, is often driven by polarised cell intercalation. Intercalation can take the

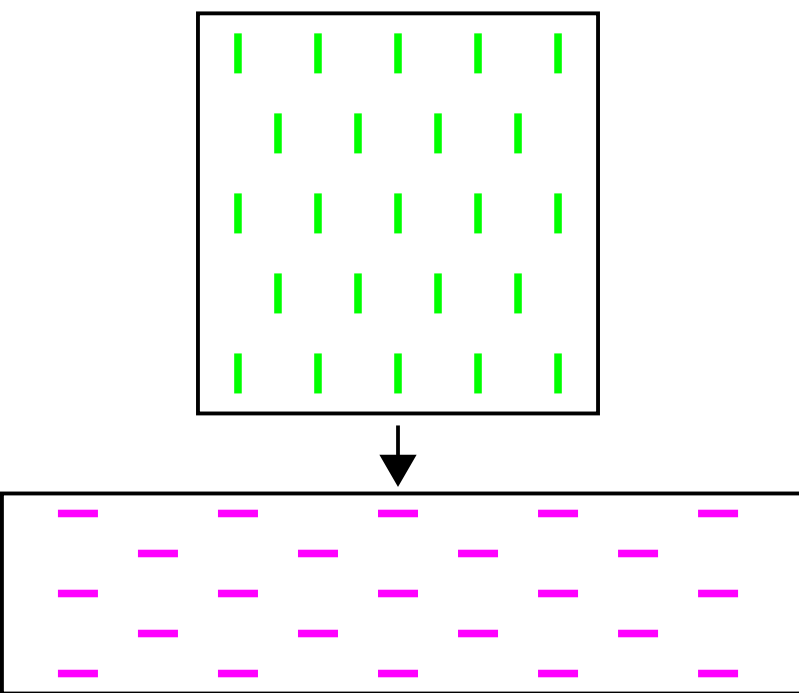
form of either a T1 Process in a tetrad of cells or the formation and resolution of a multicellular rosette. In *Drosophila*, junction shrinkage (b) is driven by planar polarised distributions of myosin II and Cadherin adhesion complexes. Cortical junctional myosin is enriched at DV-oriented shrinking junctions, while Cadherin adhesion complexes are enriched at stable AP-oriented junctions. Junction shrinkage is further driven by pulsatile flows of medial myosin, which flow into shrinking junctions. To achieve new junction growth (c), junctional myosin II activity must be reduced in the growing junction. Junctions then grow due to cell non-autonomous forces generated by medial myosin pulses in adjacent cells, close to the ends of the new junction.

Figure 3. Regulation of tissue fluidity in the *Drosophila* notum. A summary of experimental observations relating to the regulated tissue fluidity of the *Drosophila* notum (see text below schematics). This tissue can undergo a jamming transition from a fluid-like regime characterised by many intercalation events (left, shrinking junctions shown in green) and irregular packing to a solid-like regime with little intercalation and more regular hexagonal packing (right).

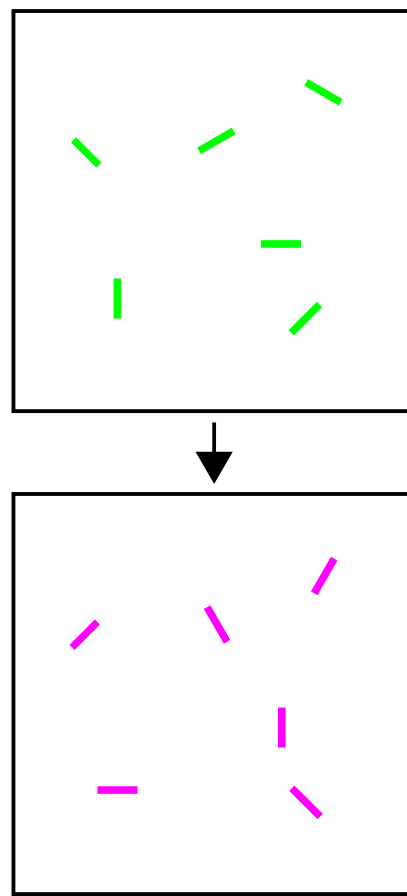
Figure 4. Vertex modelling of intercalation. (a) Schematic representation of vertex model cells (α) and junctions (ij). (b) Vertex model behaviours are determined by an energy function comprising three key terms: Cell Area Elasticity, Cell Perimeter Contractility and Junction Line Tension. (c) Implementation of intercalation in vertex models. Intercalation can arise due to either polarised line tension (top) or fluctuations in line tension around a global mean (bottom). Line tension magnitudes are indicated by the thickness of green junctions. Old neighbours are in yellow, new neighbours in grey. Intercalations occur when junctions reach a threshold short length and the rearrangement induced by an intercalation reduces the total energy. (d) Summary of vertex model terms and parameters.



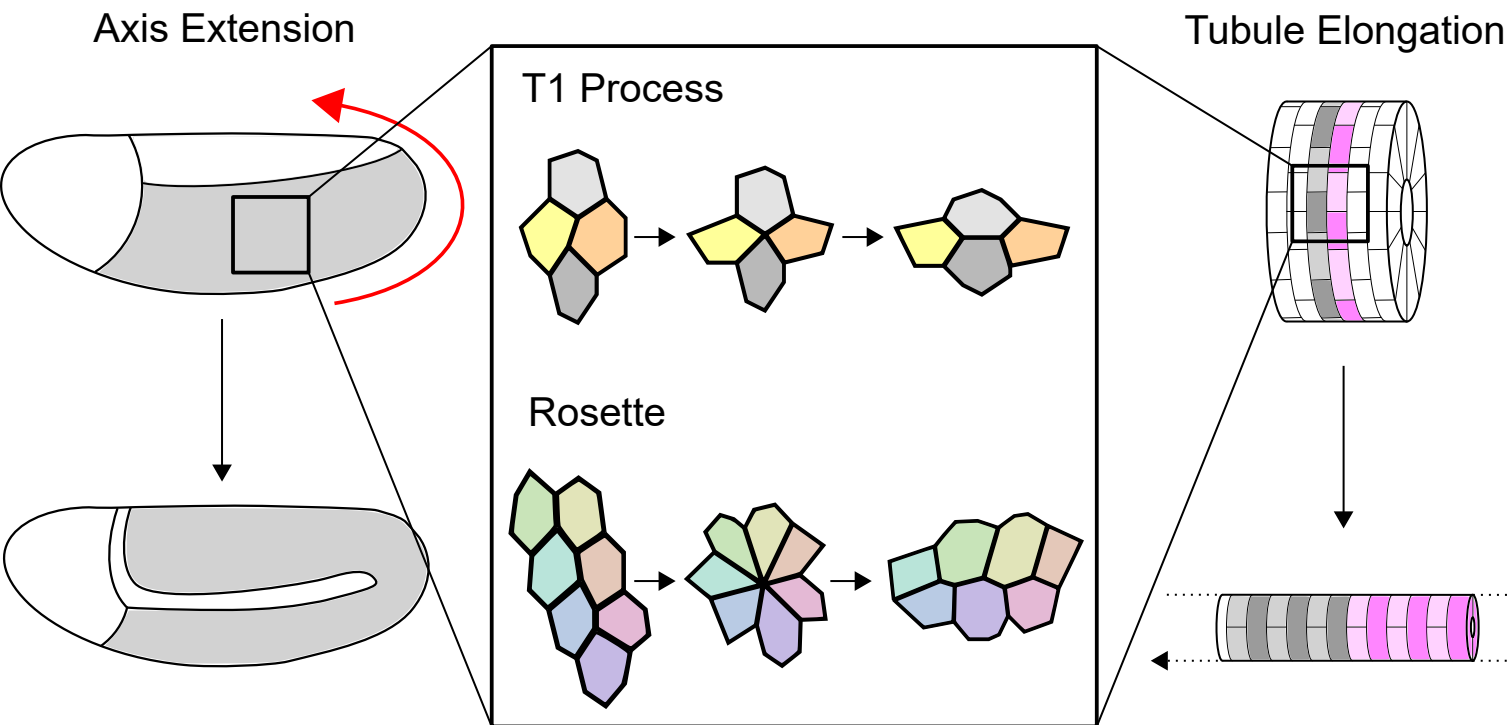
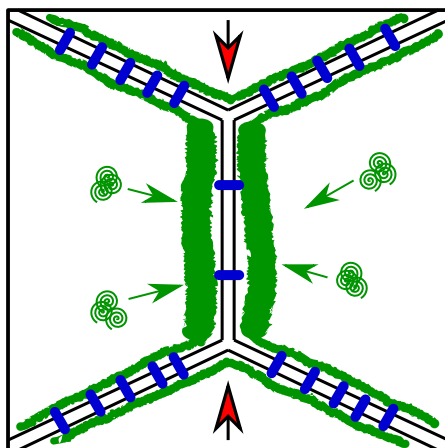
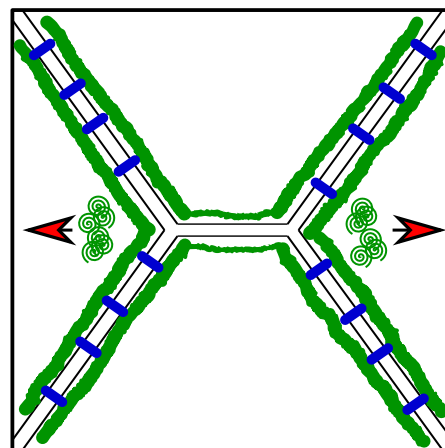
b) *Intercalation With Tissue Deformation*



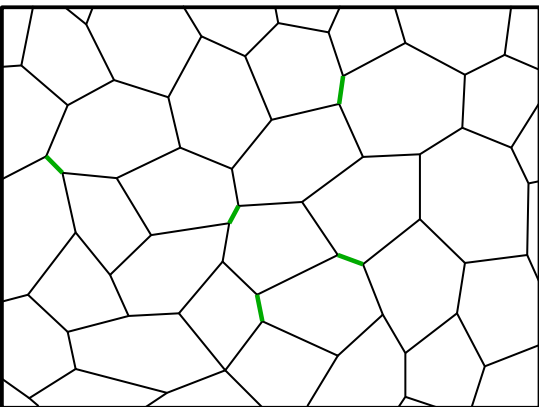
c) *Intercalation Without Tissue Deformation*
OR
"Tissue Fluidity"



a)

b) **Junction Shrinkage**c) **Junction Growth**

Fluid-like



Intercalation rate high

No change in tissue boundary

Intercalations unpolarised

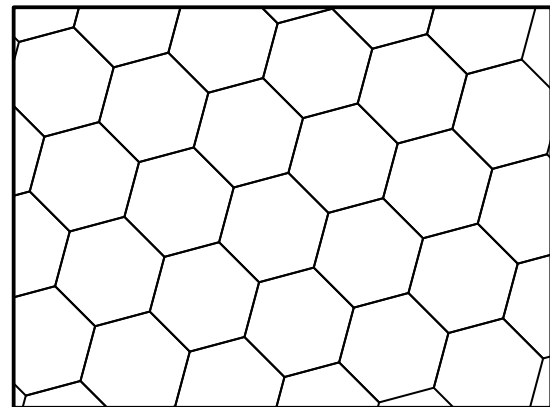
Myosin fluctuations

Tension low

Packing irregular

Jamming
Transition

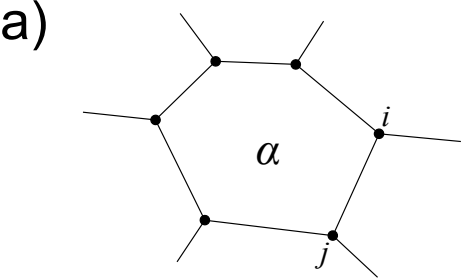
Solid-like



Intercalation rate low

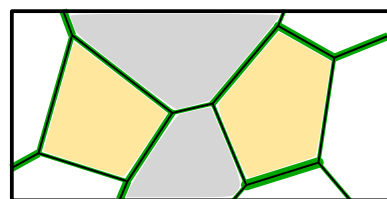
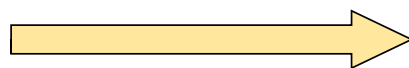
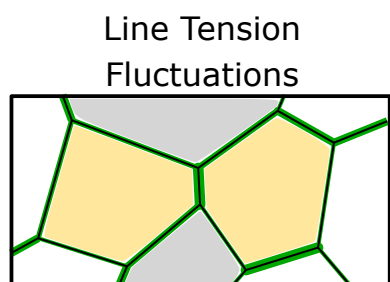
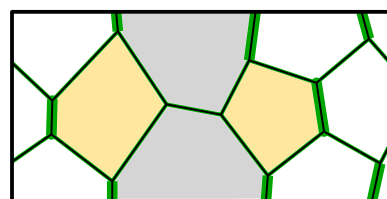
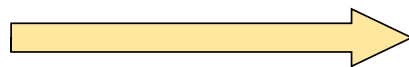
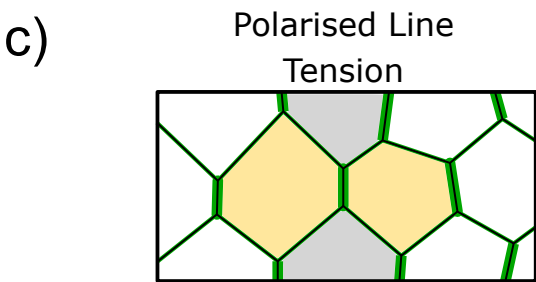
Tension high

Increased hexagonal packing



b)

$$E = \sum_{\alpha} \left[\underbrace{\frac{1}{2} K_{\alpha} (A_{\alpha} - A_{\alpha}^0)^2}_{\text{Cell Area Elasticity}} + \underbrace{\frac{1}{2} \Gamma_{\alpha} P_{\alpha}^2}_{\text{Cell Perimeter Contractility}} \right] + \sum_{\langle ij \rangle} \underbrace{\gamma_{ij} l_{ij}}_{\text{Junction Line Tension}}$$



Threshold Short
Junction Length
+
Energy Minimisation

d)

Vertex-Based Models

Cell Area Elasticity. Cells are ascribed a preferred area (A^0), which in biological terms refers to the control of apical cell area by the relationship between cell height (determined by the apicobasal polarity network) and cell volume. Cell area (A) deviations from this preferred area increase the cell area term in the energy function and any deviation is therefore minimised.

Cell Perimeter Contractility. Contractility of the cell's perimeter (P) through the activity of cortical actomyosin will lead the cell to try and reduce its perimeter. In the model, the perimeter term is therefore minimised by a reduction in perimeter length, however this will be counteracted by the preferred cell area (as logically a decrease in perimeter length will be accompanied by a decrease in cell area). The relative weights given to area elasticity and perimeter contractility in this balance, are determined by their respective coefficients (respectively K and Γ).

Junction Line Tension. While cell perimeter contractility is a "whole cell" property, the line tension term in the vertex model refers to single junctions (of length l) shared between two neighbouring cells (sometimes referred to as bicellular junctions). The addition of this term to the model has two advantages. Firstly, by ascribing different line tensions to junctions within the same cell, it is possible to introduce polarised contractility into the model. Secondly, this term can be used to describe the relative contribution of cell-cell adhesion and actomyosin contractility to line tension. Cell-cell adhesion is predicted to decrease line tension, making the term negative, while the opposite is true for contractility (determined by the coefficient γ). The total tension in a single junction is therefore the sum of the proportional perimeter contractility and line tension terms, while the ratio of Γ and γ defines the preferred perimeter of a cell.